Supported in part by

Overview of femtoscopy results from STAR experiment

Vinh Luong *(for the STAR Collaboration)*

Joint Institute for Nuclear Research

"Physics performance studies at NICA" (NICA-2024)
Online, 25–27 November 2024

Outline

- Introduction
  - Femtoscopy technique
  - STAR experiment
- Extracting emitting source
  - $\pi^{\pm}\pi^{\pm}$, $K^{\pm}K^{\pm}$, πK correlations
- Extracting final state interactions
  - $K^0_s K^{\pm}, K^0_s K^0_s, \bar{p}\bar{p}, pd, dd, d\Lambda, p\Xi^-, p\Omega^-, \Lambda\Lambda$ correlations

Femtoscopy

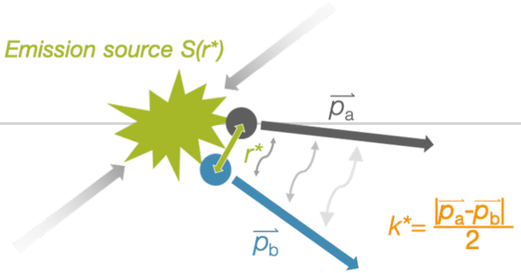

Correlation functions:

$$C(k^*) = \int S(r^*) \left| \Psi(k^*, r^*) \right|^2 d^3 r^* = \frac{A(k^*)}{B(k^*)}$$

Model — Measurement

r^*: relative distance, k^*: relative momentum

$S(r^*)$: source function

$\Psi(k^*, r^*)$: two-particle wave function

$A(k^*)$: distribution of pairs from one event, containing quantum statistical (QS) correlations, final state interactions (FSI) (Coulomb, strong)

$B(k^*)$: distribution of pairs from mixed events, served as background

- *Femtoscopy* is a powerful technique to study characteristics of systems of femtometer scale at kinetic freeze-out
- Extracting emitting source
  - If $\Psi(k^*, r^*)$ is assumed, then geometric and dynamic properties of the source can be measured
- Non-traditional femtoscopy
  - If $S(r^*)$ is assumed, then parameters of final state interactions can be determined
  - Lednický–Lyuboshitz analytical model is widely used to extract strong FSI parameters

STAR detector

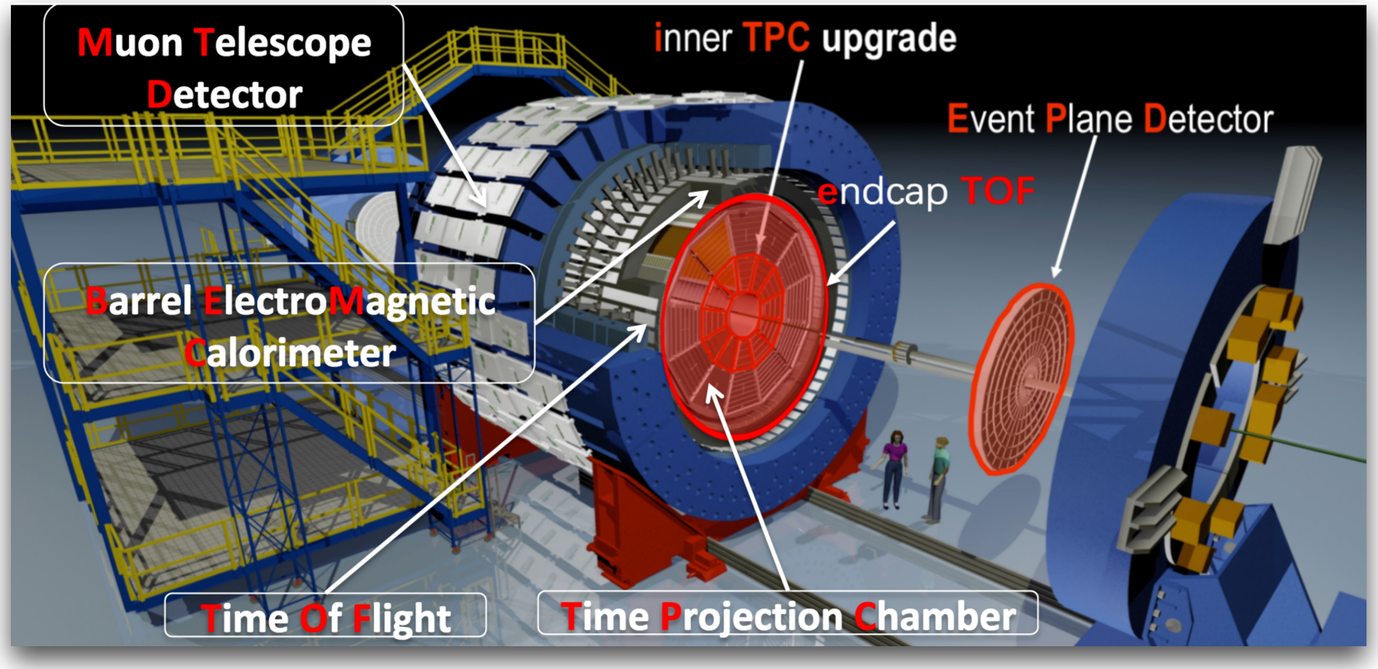

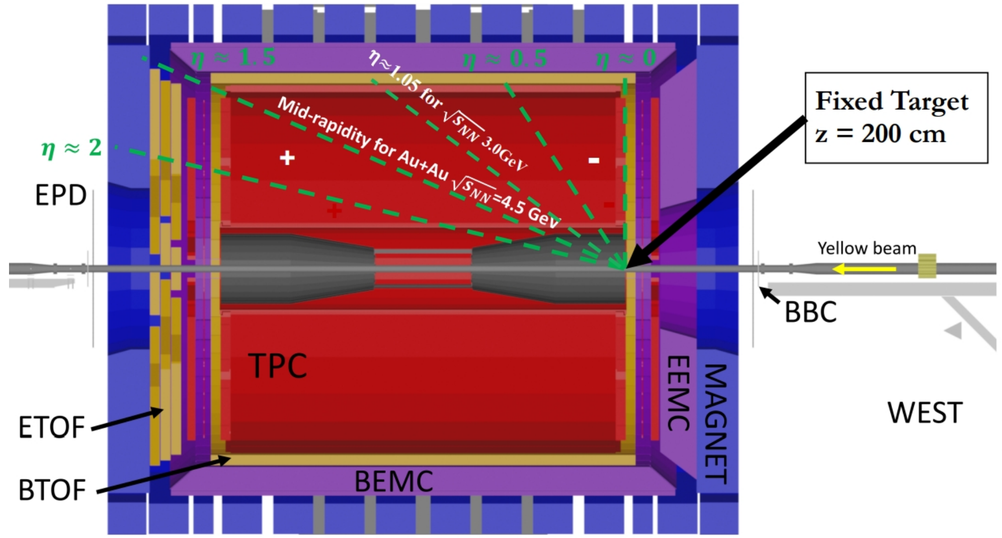

- Beam energy scan II (BES-II) upgrades
  - iTPC (2019+): extended η acceptance and improved tracking, dE/dx resolution
  - eTOF (2019+): extended PID coverage
  - EPD (2018+): EP determination away from mid-rapidity, improved EP resolution compared to BBC

- Fixed-target (FXT) setup extend energy down to $\sqrt{s_{\mathrm{NN}}}$ = 3.0 GeV

Collision systems and energies at STAR

- BES-II and FXT program: Au+Au collisions at $\sqrt{s_{\mathrm{NN}}}$ = 3.0 — 54.4 GeV
- Top RHIC energy $\sqrt{s_{\mathrm{NN}}}$ = 200 GeV:, Au+Au, Zr+Zr, Ru+Ru, p+Au, d+Au, t+Au, O+O, etc.

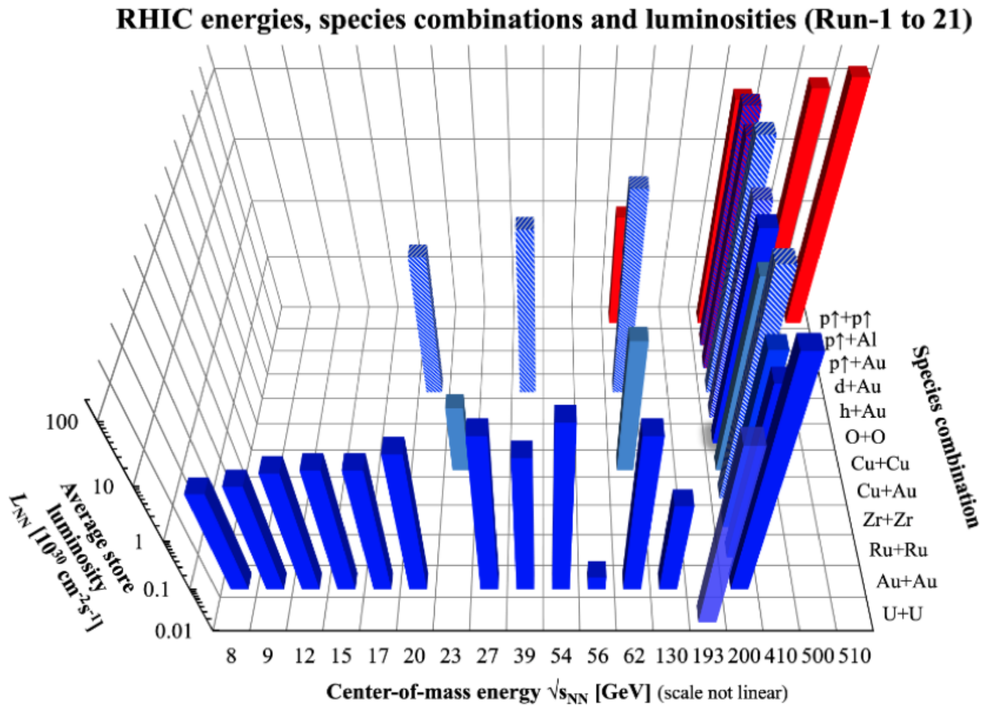

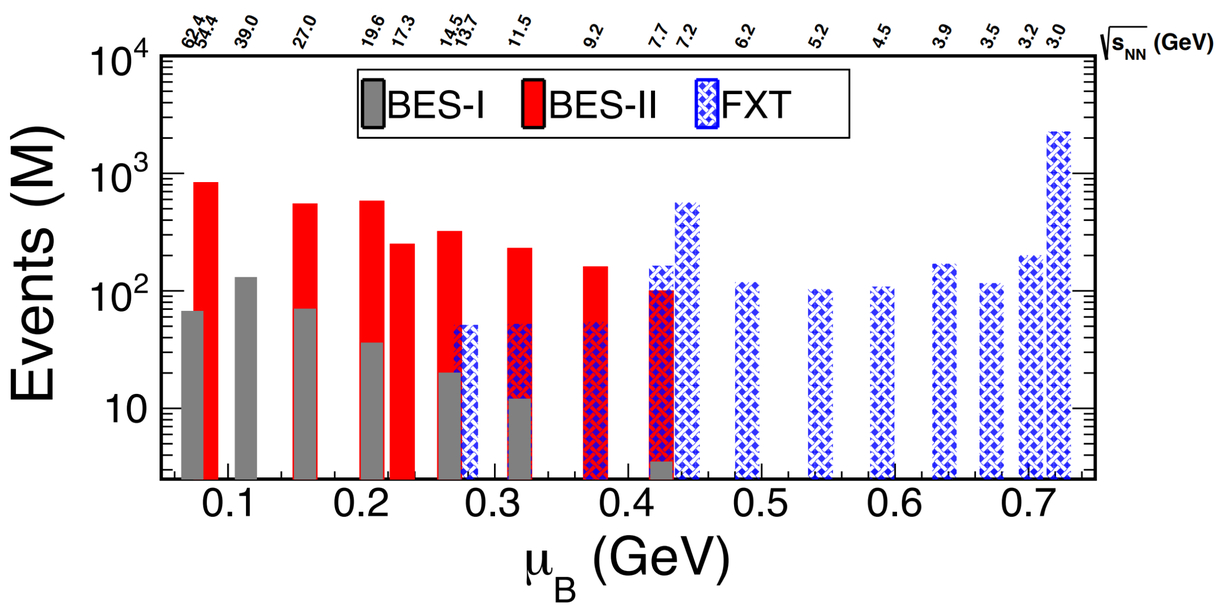

Particle identification & reconstruction

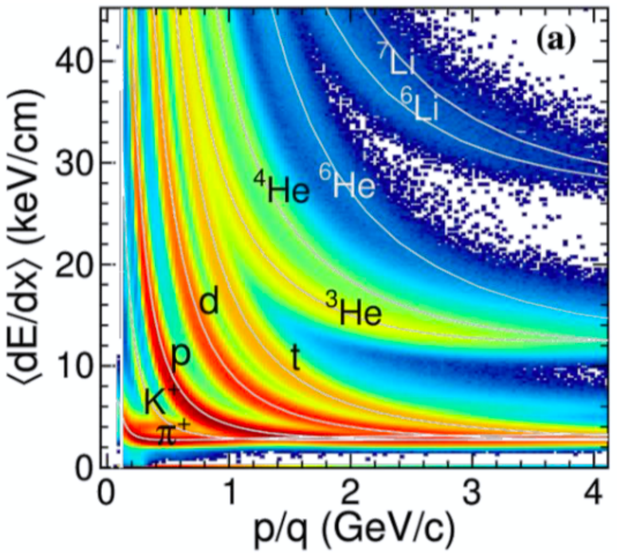

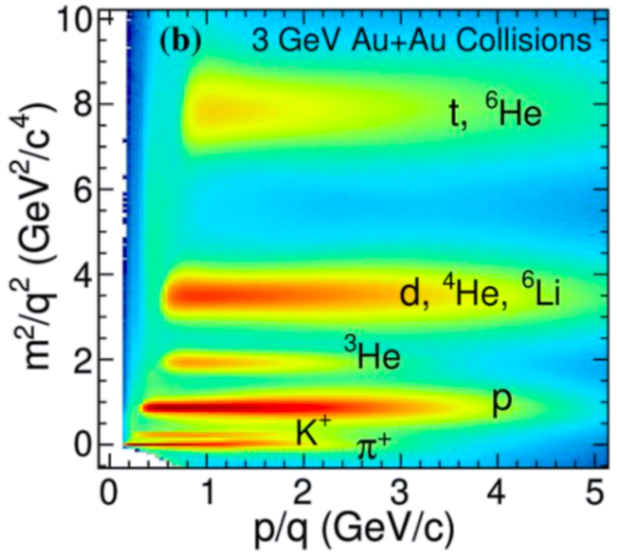

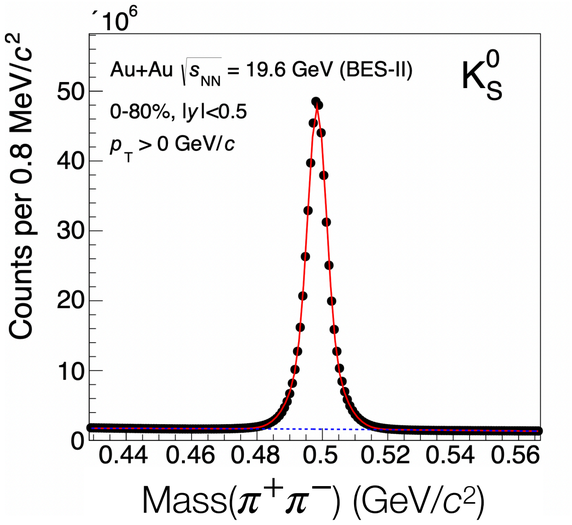

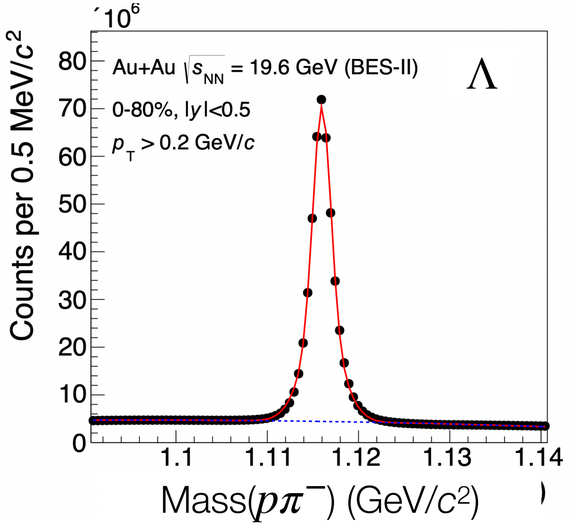

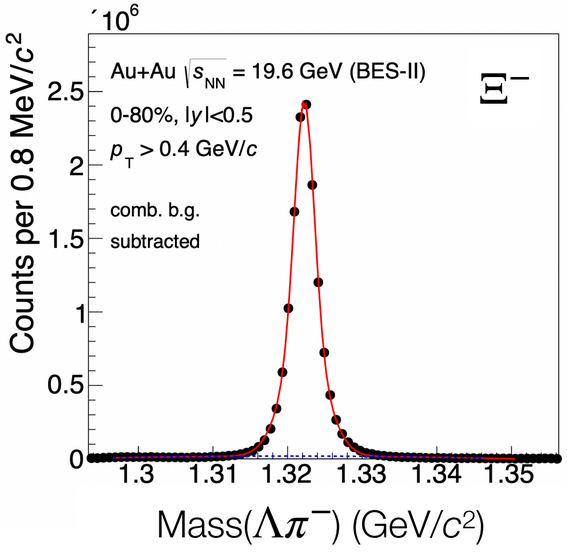

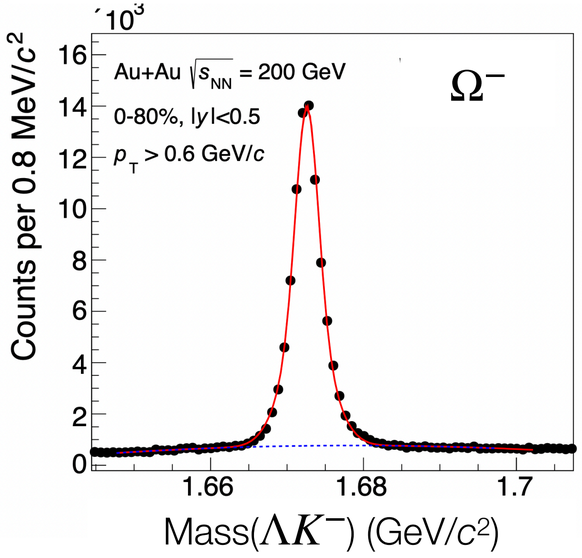

- Particle identification by TPC dE/dx and TOF m^2
- Reconstruction of short-lived particles via their decay channels
- Good particle identification and reconstruction capability

Extraction of geometric and dynamic properties of the source

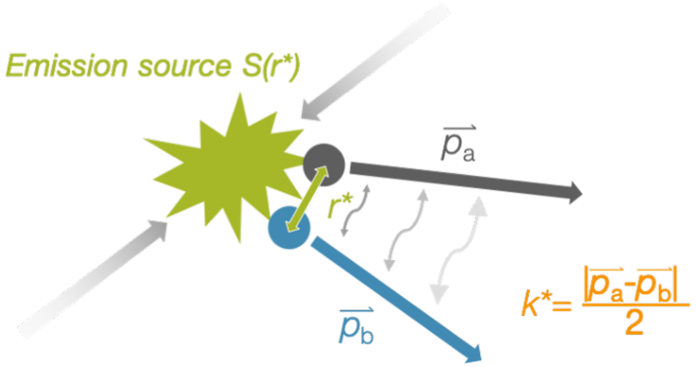

Object of study

$$C(k^*) = \int S(r^*) \left| \Psi(k^*, r^*) \right|^2 d^3 r^* = \frac{A(k^*)}{B(k^*)}$$

Model

Measurement

Charged pion/kaon femtoscopy

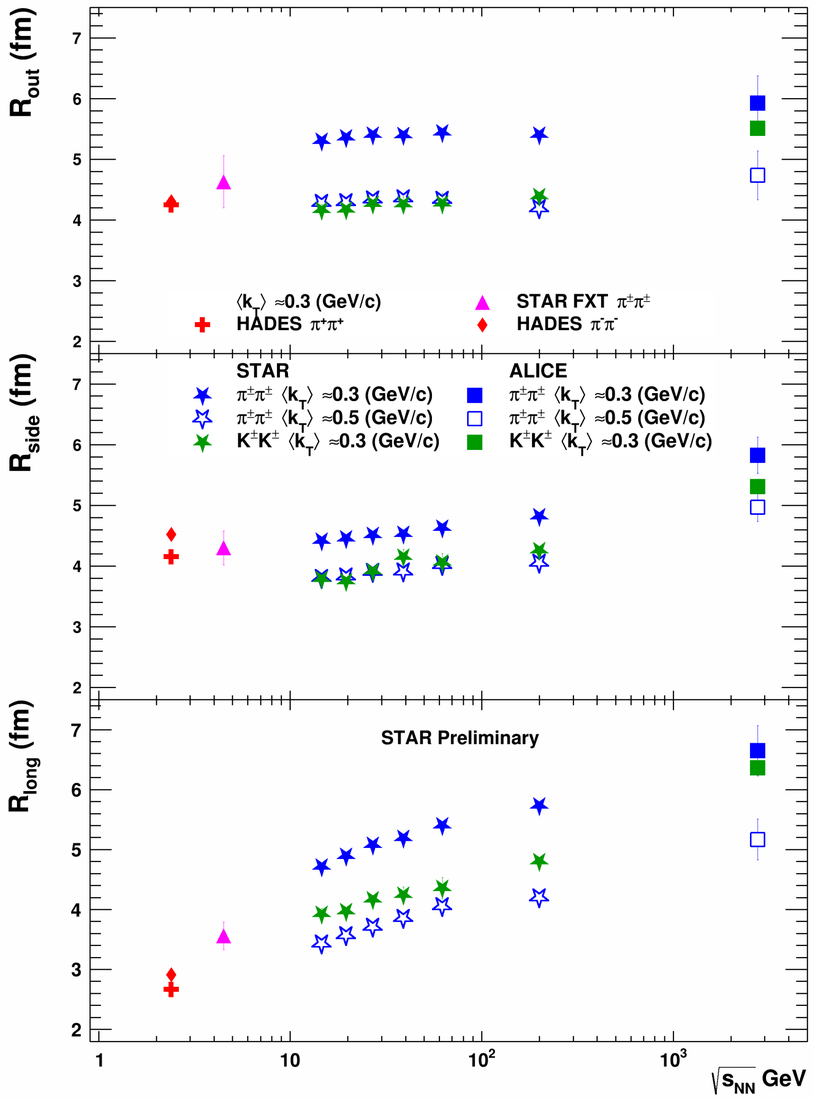

- $C(\vec{q}) = (1-\lambda) + \lambda K_{\mathrm{Coul}}(q_{\mathrm{inv}}) \times \left(1 + e^{-q_o^2 R_o^2 - q_s^2 R_s^2 - q_l^2 R_l^2}\right)$,

  where
  - $\lambda \propto$ fraction of correlated pairs
  - $R_{\mathrm{out}} \propto$ geometrical size, emission duration, and transverse flow
  - $R_{\mathrm{side}} \propto$ geometrical size
  - $R_{\mathrm{long}} \propto$ longitudinal flow, evolution time
- Femtoscopic parameters are extracted over a wide range of collision energies
- Extracted radii increase with increasing collision energy
- Extracted radii decrease with increasing transverse mass

Identical charged pion femtoscopy

Freeze-out eccentricity

Azimuthal-sensitive femtoscopy analysis:

$$R_\mu^2(\Phi) = R_{\mu,0}^2 + 2\sum_{n=2,4,6,\ldots} R_{\mu,n}^2 \cos(n\Phi),\ \mu = \mathrm{o, s, l, ol}$$

$$R_\mu^2(\Phi) = R_{\mu,0}^2 + 2\sum_{n=2,4,6,\ldots} R_{\mu,n}^2 \sin(n\Phi),\ \mu = \mathrm{os}$$

Kinetic freeze-out eccentricity:

$$\varepsilon_\mathrm{F} = \frac{\sigma_y'^2 - \sigma_x'^2}{\sigma_y'^2 + \sigma_x'^2} \approx 2\frac{R_{s,2}^2}{R_{s,0}^2}$$

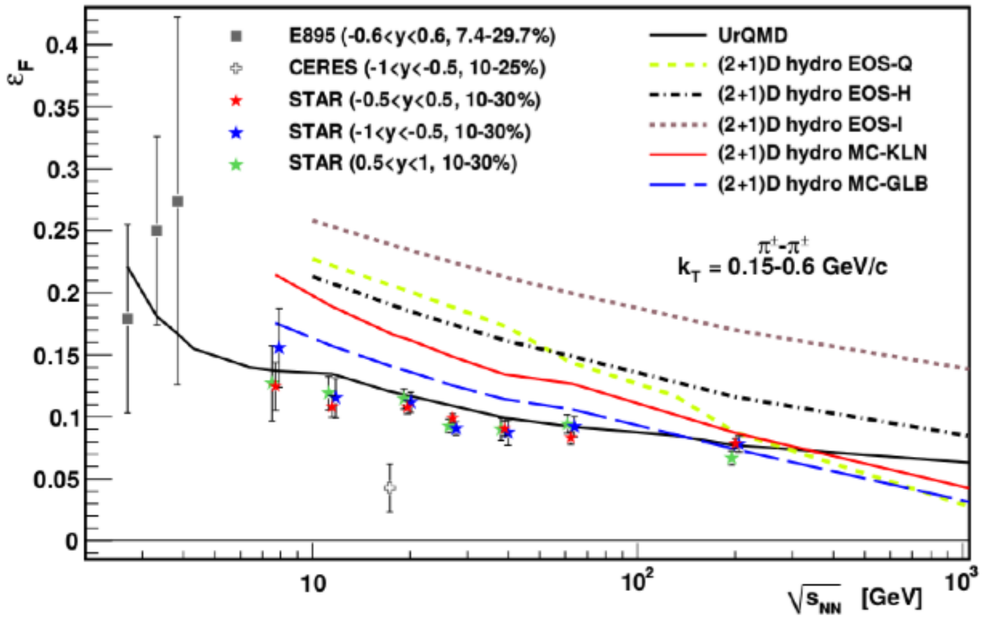

- ε_F decreases with beam energy
  - Consistent with expectation at higher energies: increased flow and/or increased lifetime

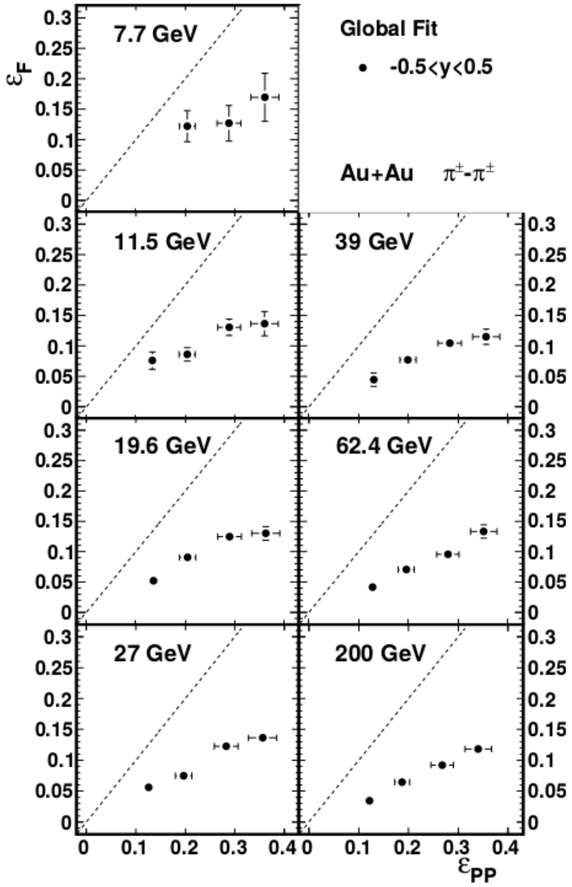

- The freeze-out shape remains an out-of-plane extended ellipse ($\varepsilon_\mathrm{F} > 0$)

STAR, Phys. Rev. C **92** (2015) 014904

Identical charged pion femtoscopy

Source tilt angle at freeze-out

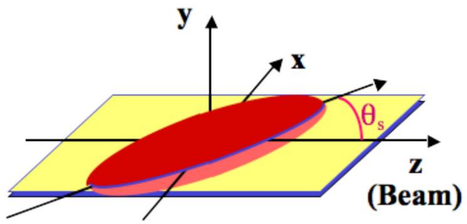

$$\theta_{\mathrm{sl}} = \frac{1}{2}\tan^{-1}\left(\frac{-R^2_{sl,1}}{R^2_{l,0} - R^2_{s,0} + 2R^2_{s,2}}\right)$$

$$\theta_{\mathrm{ol}} = \frac{1}{2}\tan^{-1}\left(\frac{-R^2_{ol,1}}{R^2_{l,0} - R^2_{s,0} + 2R^2_{s,2}}\right)$$

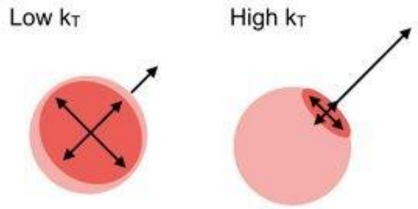

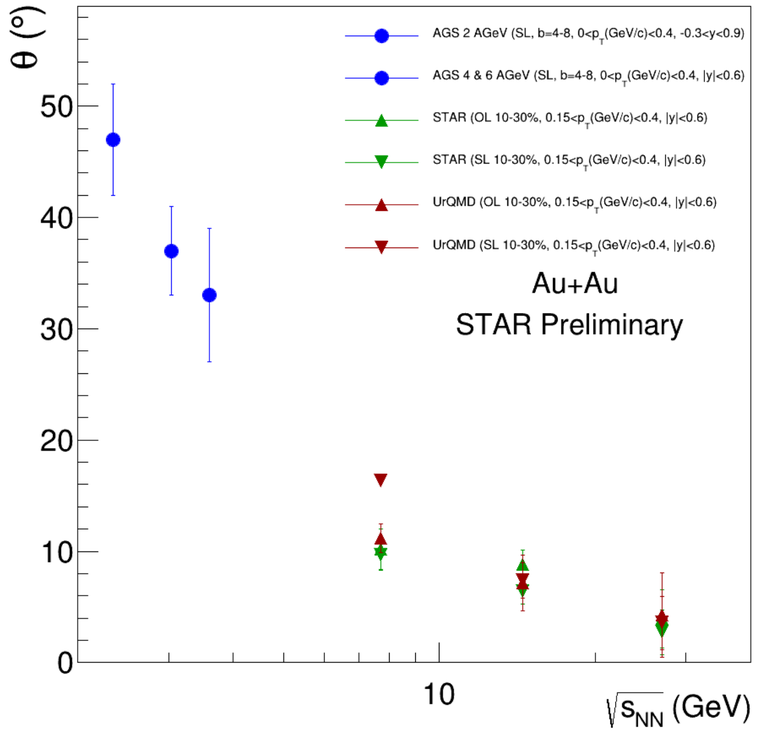

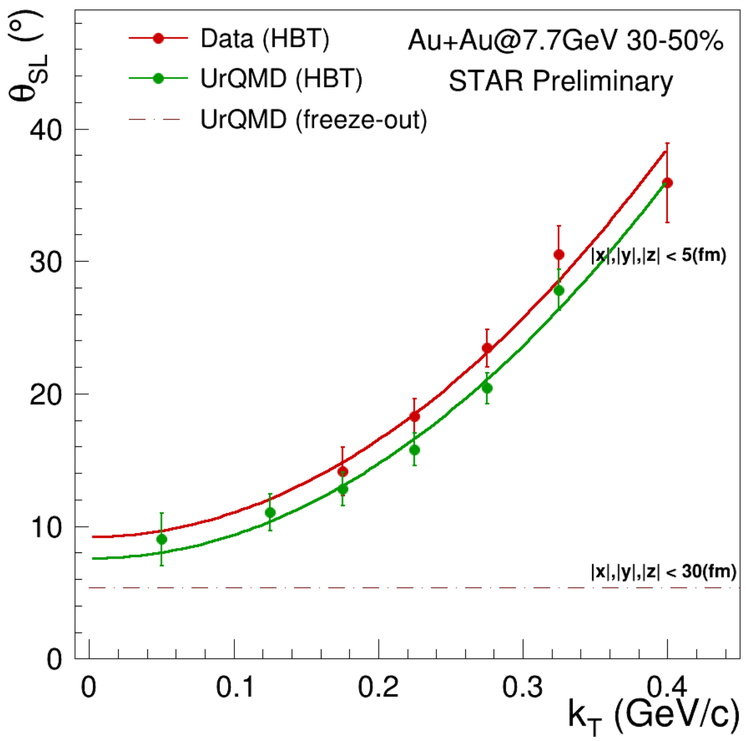

- The source tilt is sensitive to the dynamical response of the strongly-interacting matter under extreme conditions
- UrQMD model quantitatively describes the results
- $\sqrt{s_{\mathrm{NN}}}$-dependence
  - In trend with AGS data
- k_{T}-dependence
  - The tilt is extrapolated to $k_{\mathrm{T}} = 0$
  - Good agreement between $\theta_{k_{\mathrm{T}}=0}$ from femtoscopy and the tilt extracted from freeze-out coordinates in UrQMD

Identical pion femtoscopy

Rapidity dependence

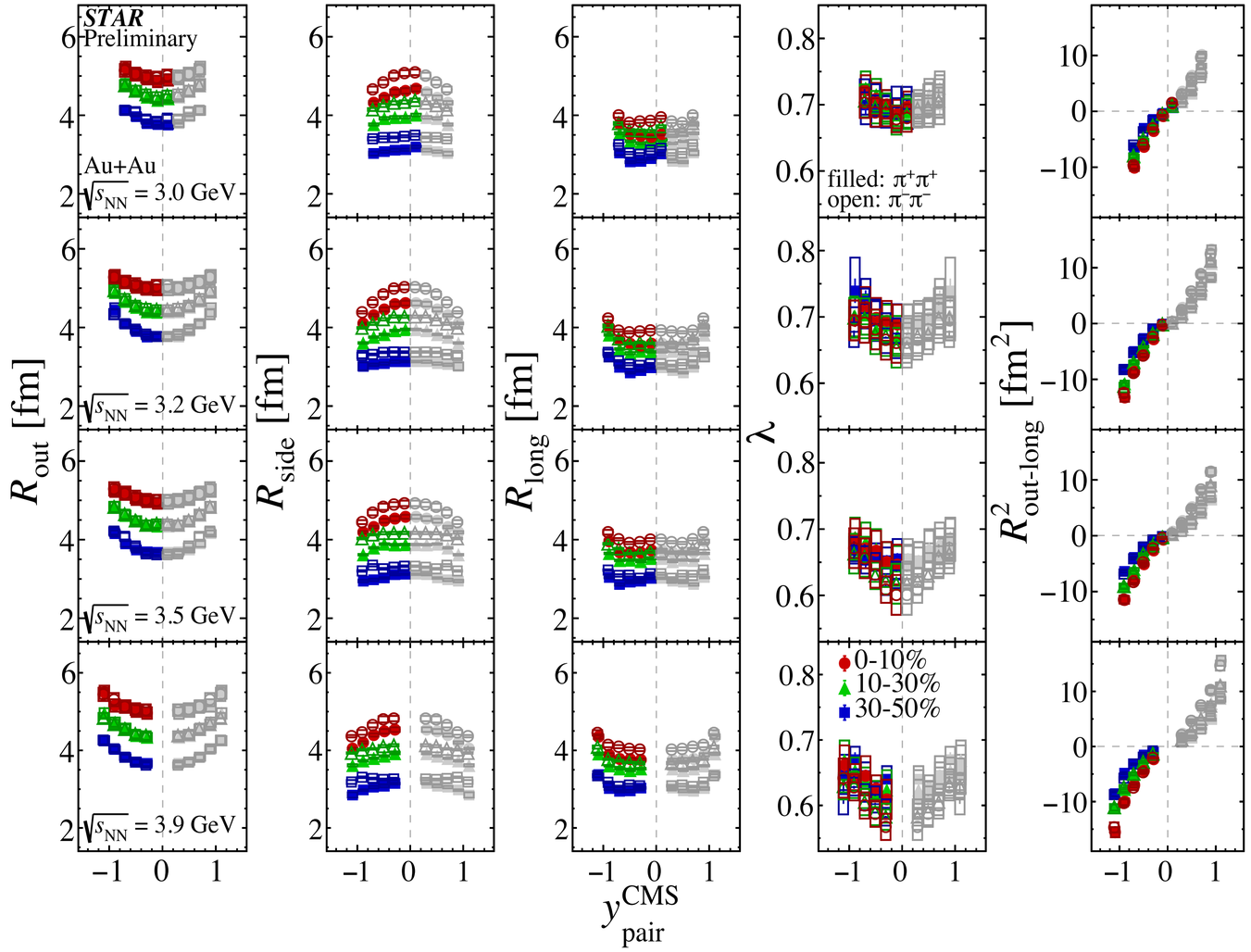

- Clear rapidity dependence of extracted femtoscopic parameters at low $\sqrt{s_{NN}}$
- Decrease of R_{side} from midrapidity to backward rapidity; non-vanishing $R^2_{out-long}$ cross-term
  - Hint of boost-invariance breaking at low $\sqrt{s_{NN}}$

Phys. Part. Nucl. **55** (2024) 822

Identical pion femtoscopy

Residual third-body Coulomb effect

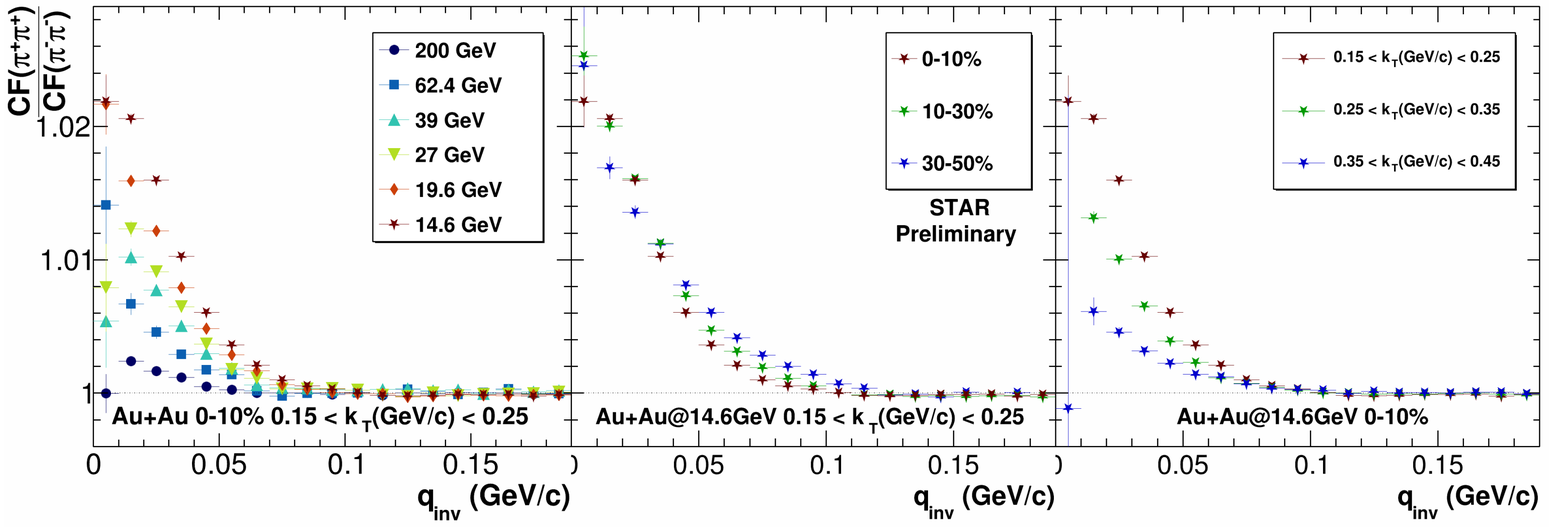

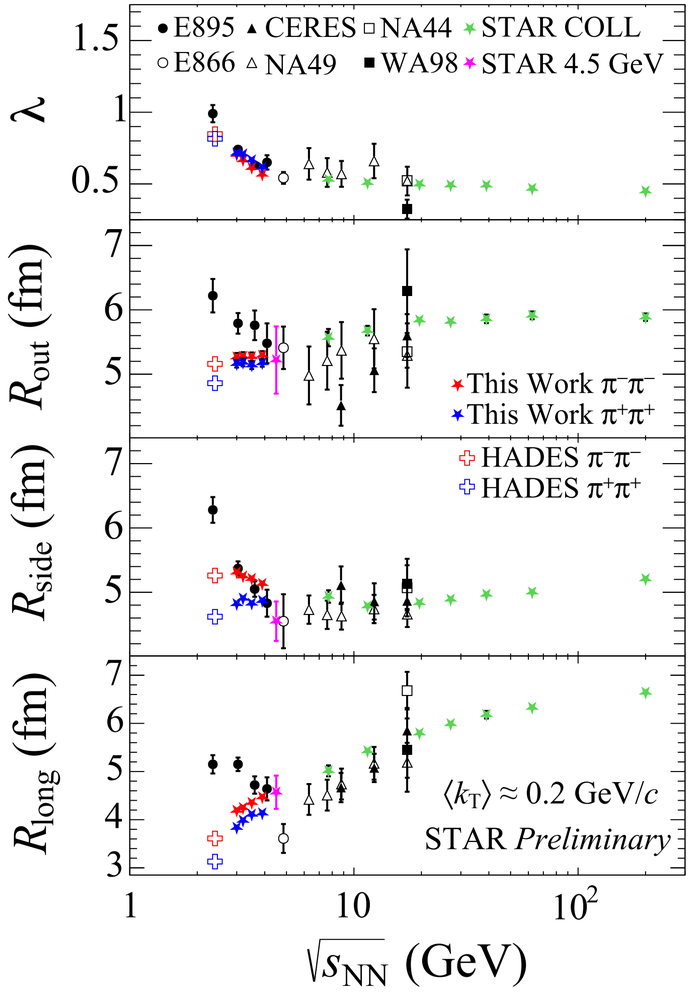

- Difference in correlation functions and extracted radii between $\pi^+\pi^+$ and $\pi^-\pi^-$ for low k_T at low $\sqrt{s_{NN}}$
  - May be attributed to residual third body Coulomb and initial isospin asymmetry

Phys. Part. Nucl. **55** (2024) 822

Two-kaon femtoscopy

Emission time

- Femtoscopy of kaons is complementary to one of pions
  - less contribution from resonances decay
  - smaller rescattering cross-section

Eq. (Y): $R_{\text{long}} = \tau\sqrt{\frac{T}{m_{\text{T}}}\frac{K_2(m_{\text{T}}/T)}{K_1(m_{\text{T}}/T)}}$

Eq. (X): $R^2_{\text{long}} = \tau^2_{\text{max}}\frac{T_{\text{max}}}{m_{\text{T}}\cosh y_{\text{T}}}\left(1+\frac{3T_{\text{max}}}{2m_{\text{T}}\cosh y_{\text{T}}}\right)$

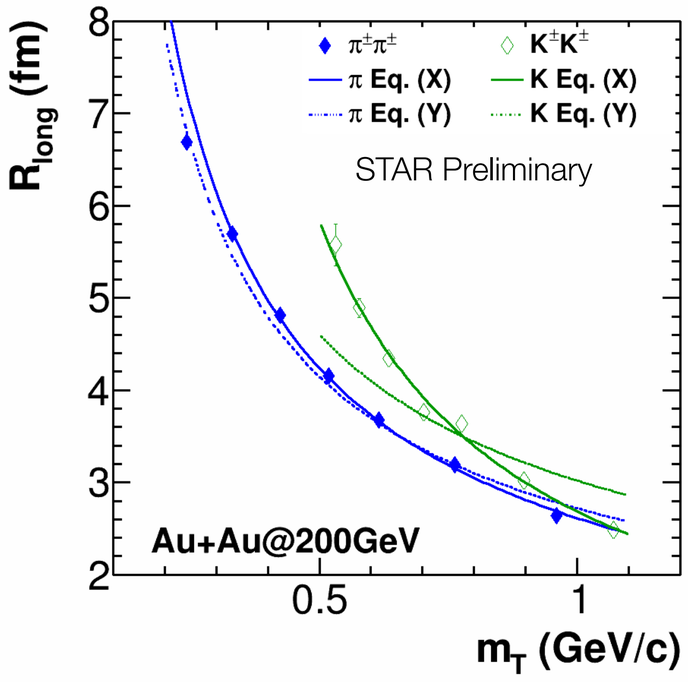

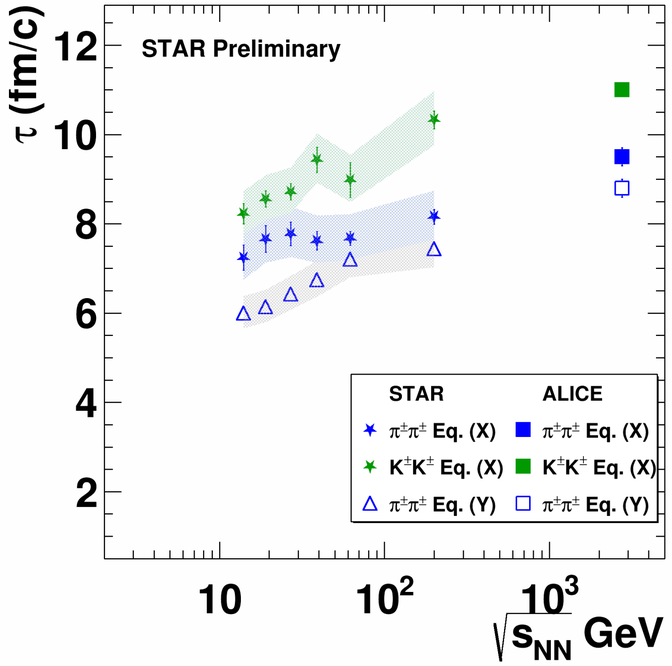

- For kaons, Eq. (Y), where transverse flow is absent, fails to describe R_{long}
- Emission time increases with increasing $\sqrt{s_{\text{NN}}}$
- Kaons are emitted later than pions → influence from K^* resonance decay

Two-kaon femtoscopy

m_T-scaling

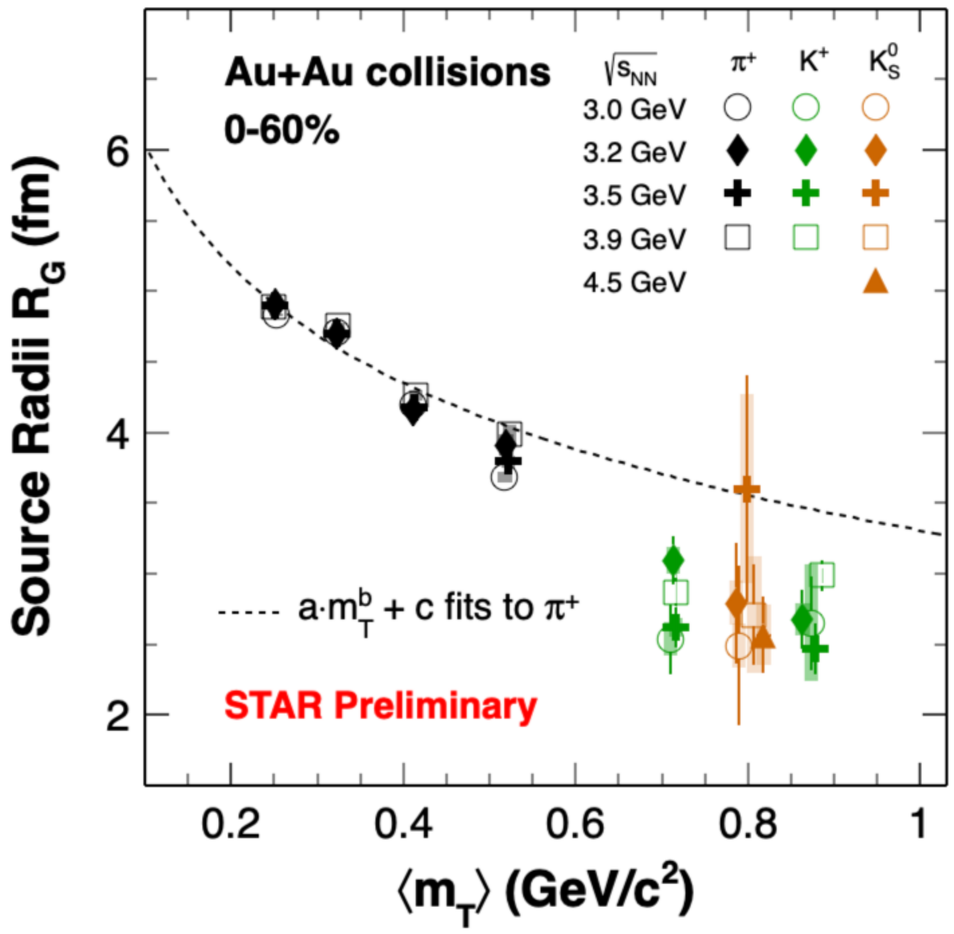

- Source size of kaons do not follow the m_T-scaling obtained from fit of pions
  - Implication of no equilibrium between pions and kaons at high baryon density

Space-time asymmetry in emission process

$C_+(k^*)$, $C_-(k^*)$: sign index reflecting the sign of $\vec{v} \cdot \vec{k_\pi^*}$

$\vec{v}$: pair velocity, $\vec{k_\pi^*}$: pion momentum in pair rest frame

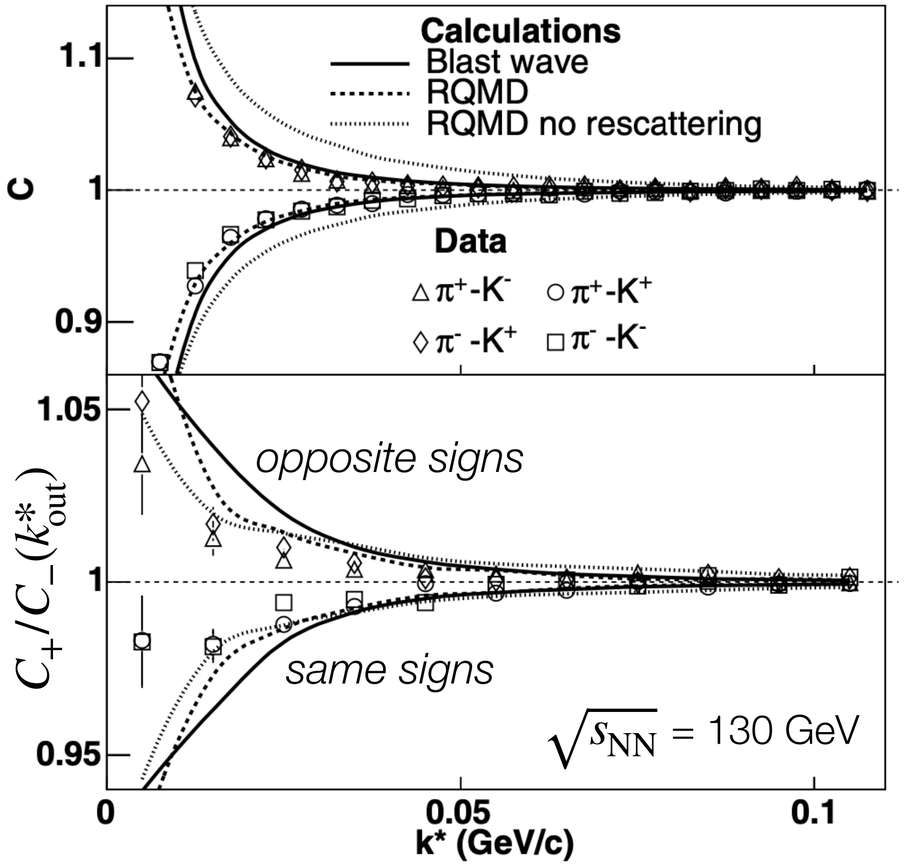

$$C_l^m(k^*) = \int C(k^*, \theta, \phi) Y_l^m(\theta, \phi) d\Omega$$

Ω: full solid angle, $Y_l^m(\theta, \phi)$: spherical harmonic functions, $k^* = |\mathbf{k}^*|$

θ, ϕ: polar and azimuthal angles

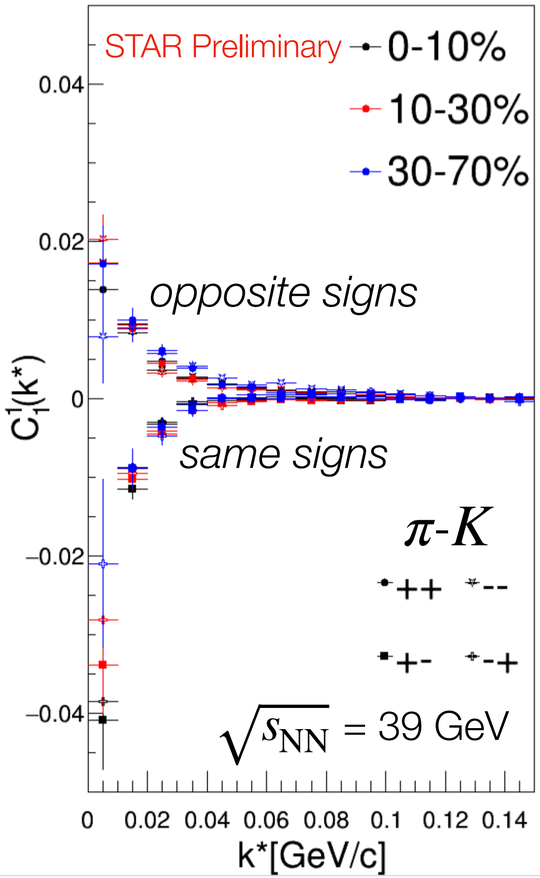

- C_+/C_- ratio and C_1^1 component of spherical harmonics decomposition are sentisitive to the emission asymmetry
- Deviation of C_+/C_- from 1 and C_1^1 from 0 suggests emission asymmetry
  - Pions are emitted closer to the center of the source and/or later than kaons

STAR, PRL **91** (2003) 262302
Nucl. Phys. A **982** (2019) 359

Source imaging

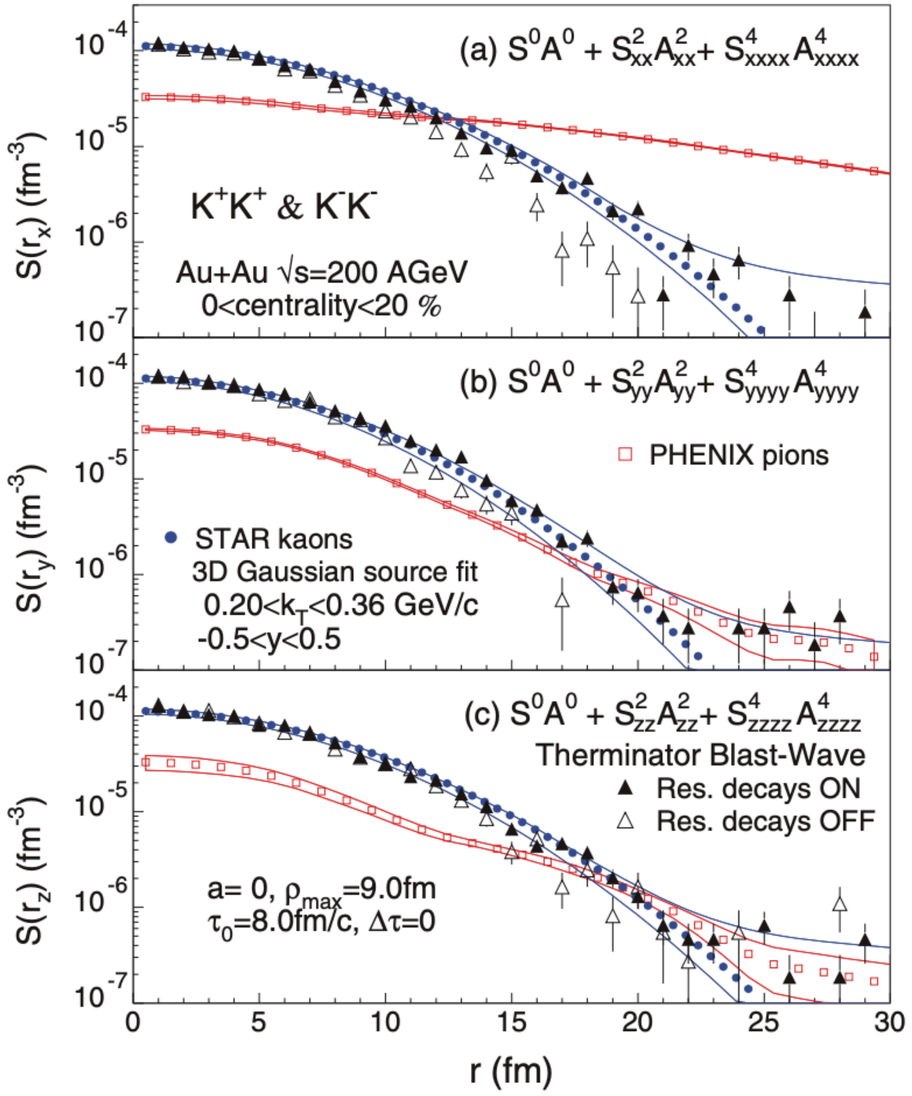

- Kaon 3D source function is extracted via the method of Cartesian surface-spherical harmonic decomposition
- 3D source function shapes for kaons and pions are different
- Source shape observed for the kaons is narrower than that of pions
  - Small role of long-lived resonance decays and/or of the exponential emission duration width $\Delta\tau$ on kaon emission

P. Danielewicz, S. Pratt, PLB 618 (2005) 60
P. Danielewicz, S. Pratt, PRC 75 (2007) 034907
STAR, PRC **88** (2013) 034906

Extraction of final state interactions

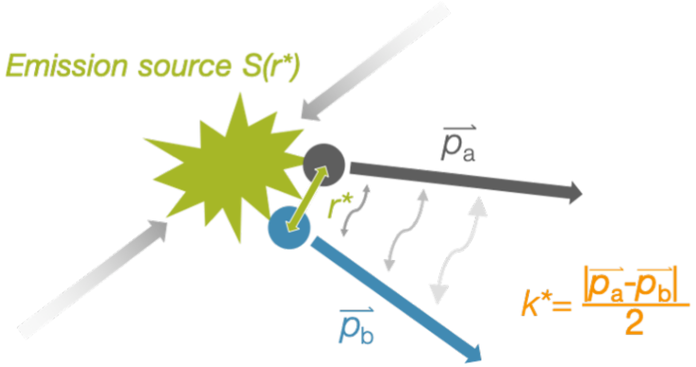

Object of study

$$C(k^*) = \int S(r^*) \left| \Psi(k^*, r^*) \right|^2 d^3 r^* = \frac{A(k^*)}{B(k^*)}$$

Model

Measurement

Neutral kaon femtoscopy

- Correlation functions can be described by Lednický–Lyuboshitz model:
  - $K_s^0 K_s^0$: QS and strong FSI due to $a_0(980)$ and $f_0(980)$ resonances

$$C(q_{inv}) = 1 + \lambda\left(e^{-R_{inv}^2 q_{inv}^2} + \frac{1}{2}\left[\left|\frac{f(k^*)}{R_{inv}}\right| + \frac{4\Re f(k^*)}{\sqrt{\pi}R_{inv}}F_1(q_{inv}R_{inv}) - \frac{2\Im f(k^*)}{R_{inv}}F_2(q_{inv}R_{inv})\right]\right)$$

  - $K_s^0 K^{\pm}$: strong FSI due to $a_0(980)$ resonance

$$C(k^*) = 1 + \frac{\lambda}{4}\left[\left|\frac{f(k^*)}{R}\right| + \frac{4\Re f(k^*)}{\sqrt{\pi}R}F_1(2k^*R) - \frac{2\Im f(k^*)}{R}F_2(2k^*R)\right]$$

Analytic functions: $F_1(z) = \int_0^z dx \frac{e^{x^2} - x^2}{z}$, $F_2(z) = \frac{1 - e^{x^2}}{z}$

$f(k^*)$: s-wave scattering amplitude

$$q_{inv} = \sqrt{(\overrightarrow{p_1} - \overrightarrow{p_2})^2 - (E_1 - E_2)^2}$$

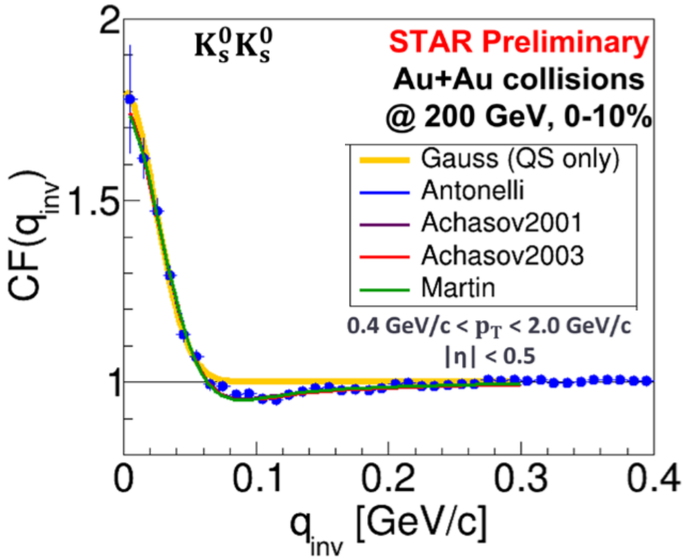

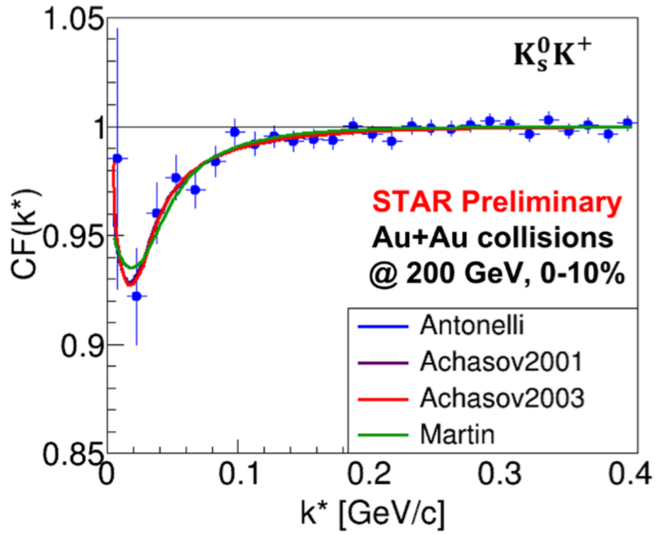

- K_s^0-K_s^0 correlation functions cannot be described by pure QS effect
  - Final state strong interaction significantly affects K_s^0-K_s^0 correlations due to two near-threshold resonances $a_0(980)$ and $f_0(980)$
- K_s^0-K^+ correlation functions is reproduced by parametrization with $a_0(980)$ resonance

R. Lednický, V.L. Lyuboshitz, Sov. J. Nucl. Phys. **35** (1982) 770
EPJ Web Conf. **276** (2023) 01016

Neutral kaon femtoscopy

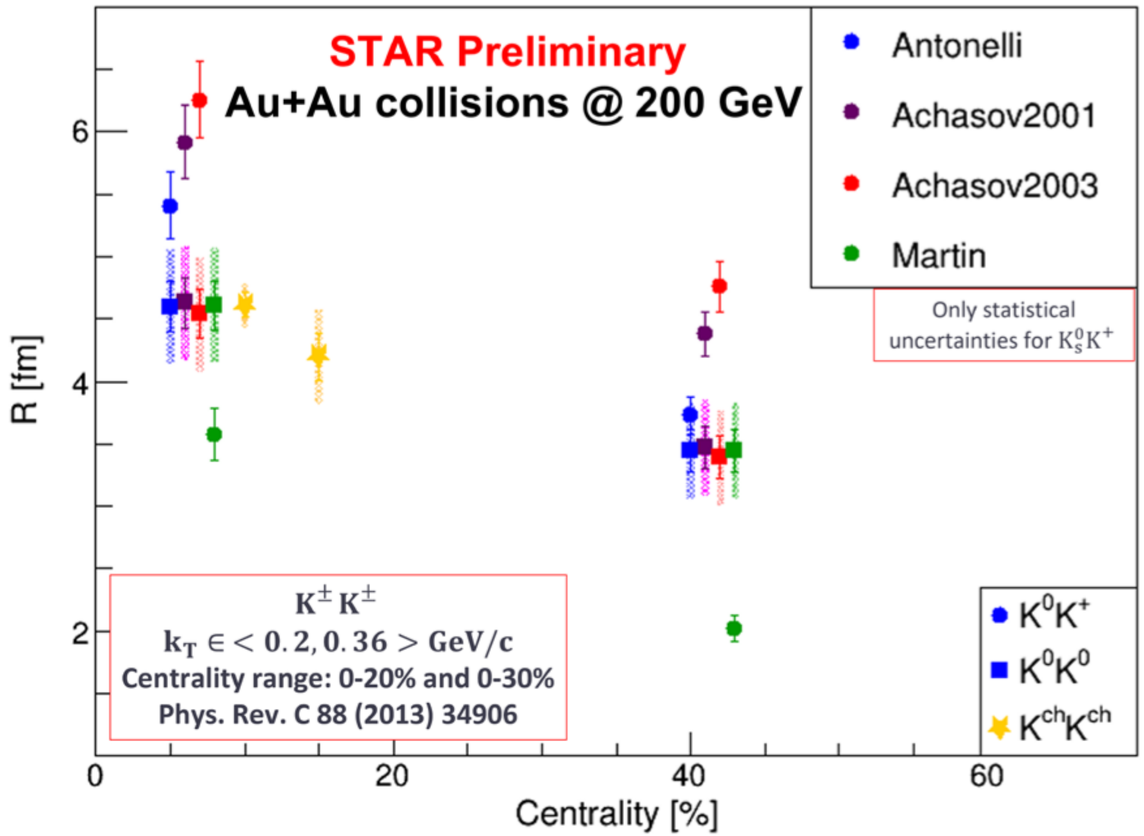

- Obtained source sizes for Antonelli parametrization are consistent among all the kaon combinations
- Antonelli parametrization favors $a_0(980)$ resonance as a tetraquark
  - $a_0(980)$ could be a tetraquark

EPJ Web Conf. **276** (2023) 01016

Antiproton-antiproton correlations

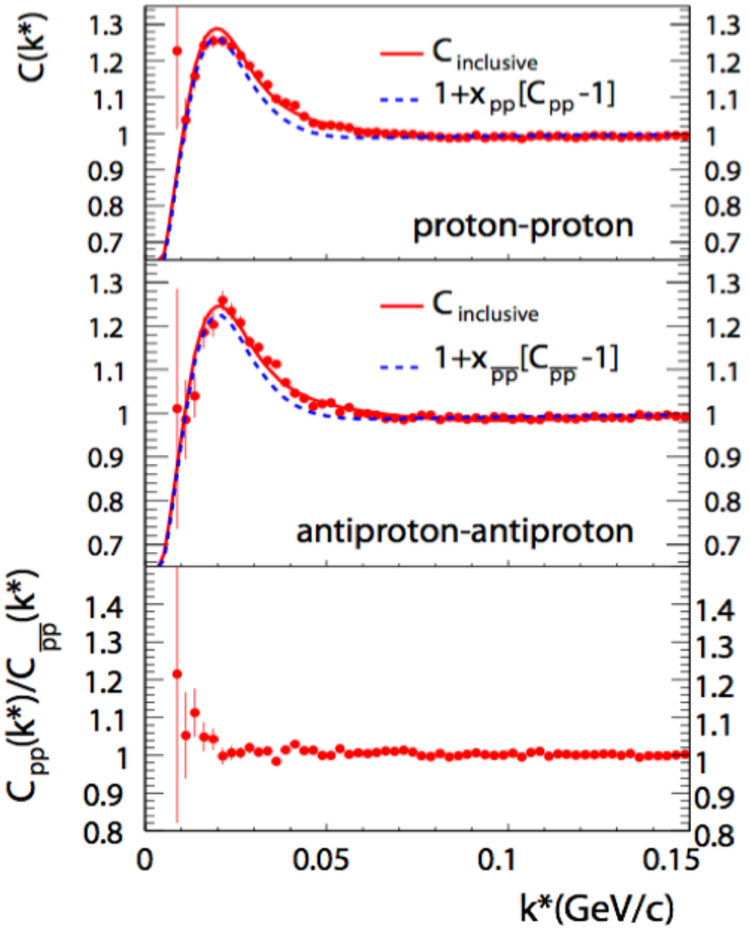

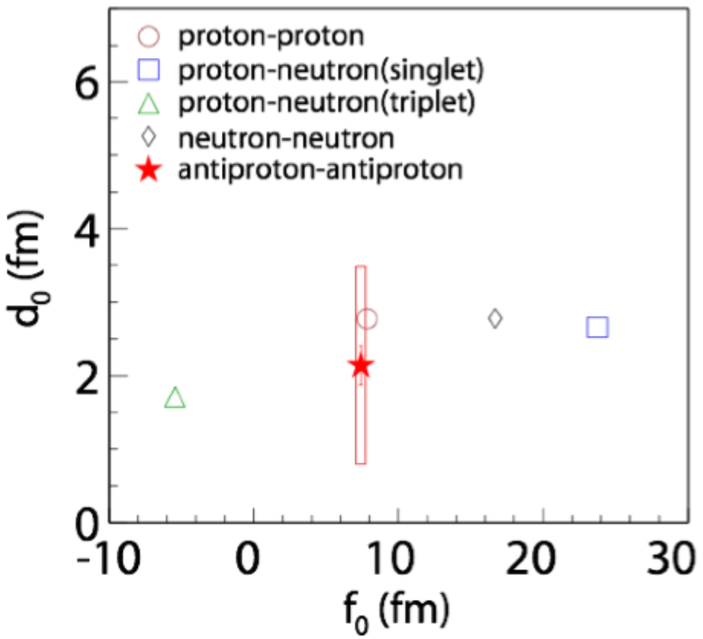

- First measurement of $\bar{p}\bar{p}$ strong interaction parameters
- f_0 and d_0 extracted from fit of correlation functions using Lednický–Lyuboshitz model for the $\bar{p}\bar{p}$ interaction is consistent with parameters for the pp interaction
  - A quantitative verification of matter-antimatter symmetry in context of the forces responsible for the binding of (anti)nuclei

R. Lednický, V.L. Lyuboshitz, Sov. J. Nucl. Phys. **35** (1982) 770
STAR, Nature **527** (2015) 345

p-d, d-d correlations

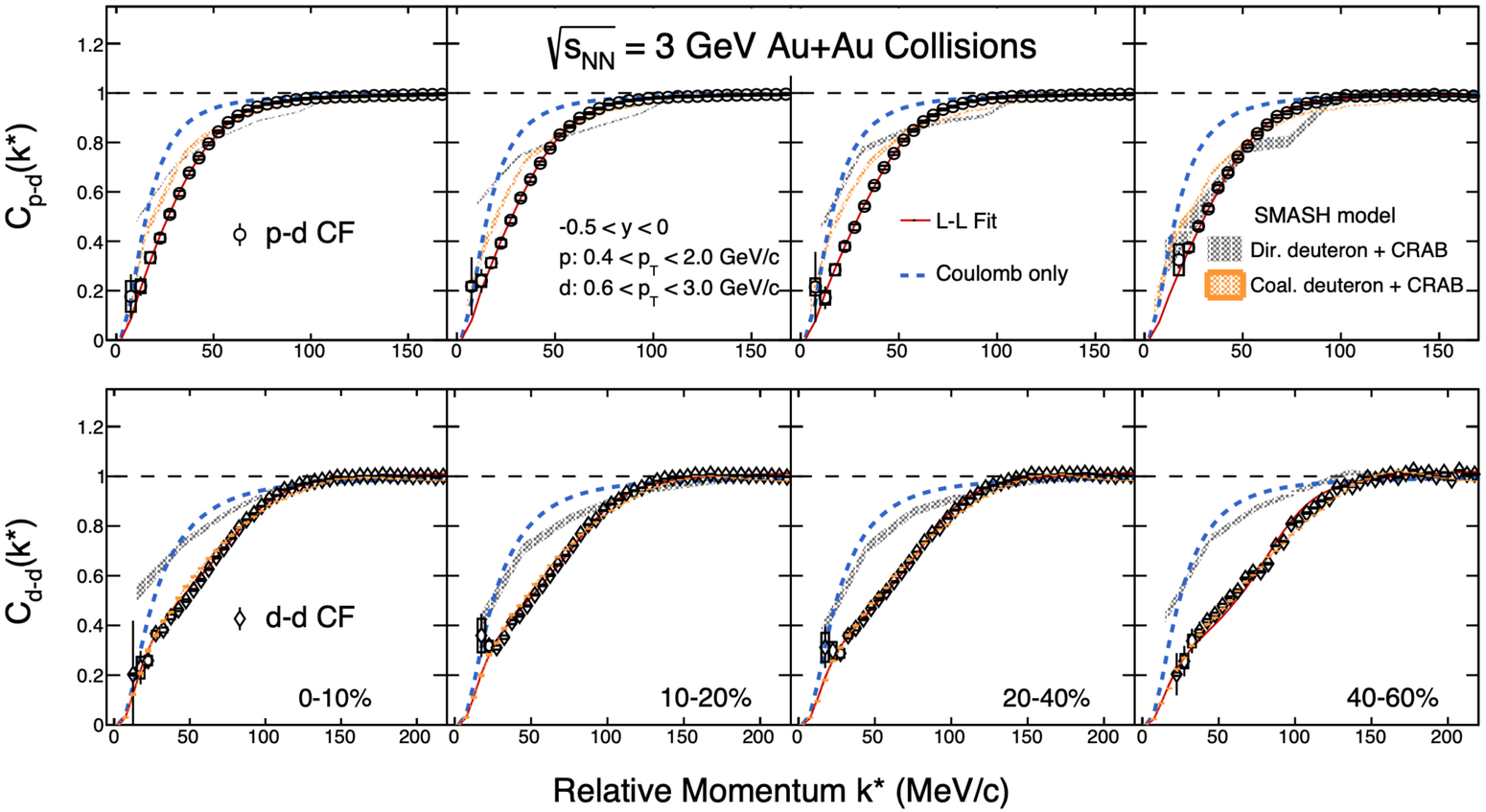

- First measurements of p-d, d-d correlation functions
- SMASH model with coalescene production of deutron describes data well
  - Coalescene is the dominant process for deuteron formation in high-energy nuclear collisions

W. Zhao et al., PRC **98** (2018) 054905
STAR, arXiv: 2410.03436

p-d, d-d correlations

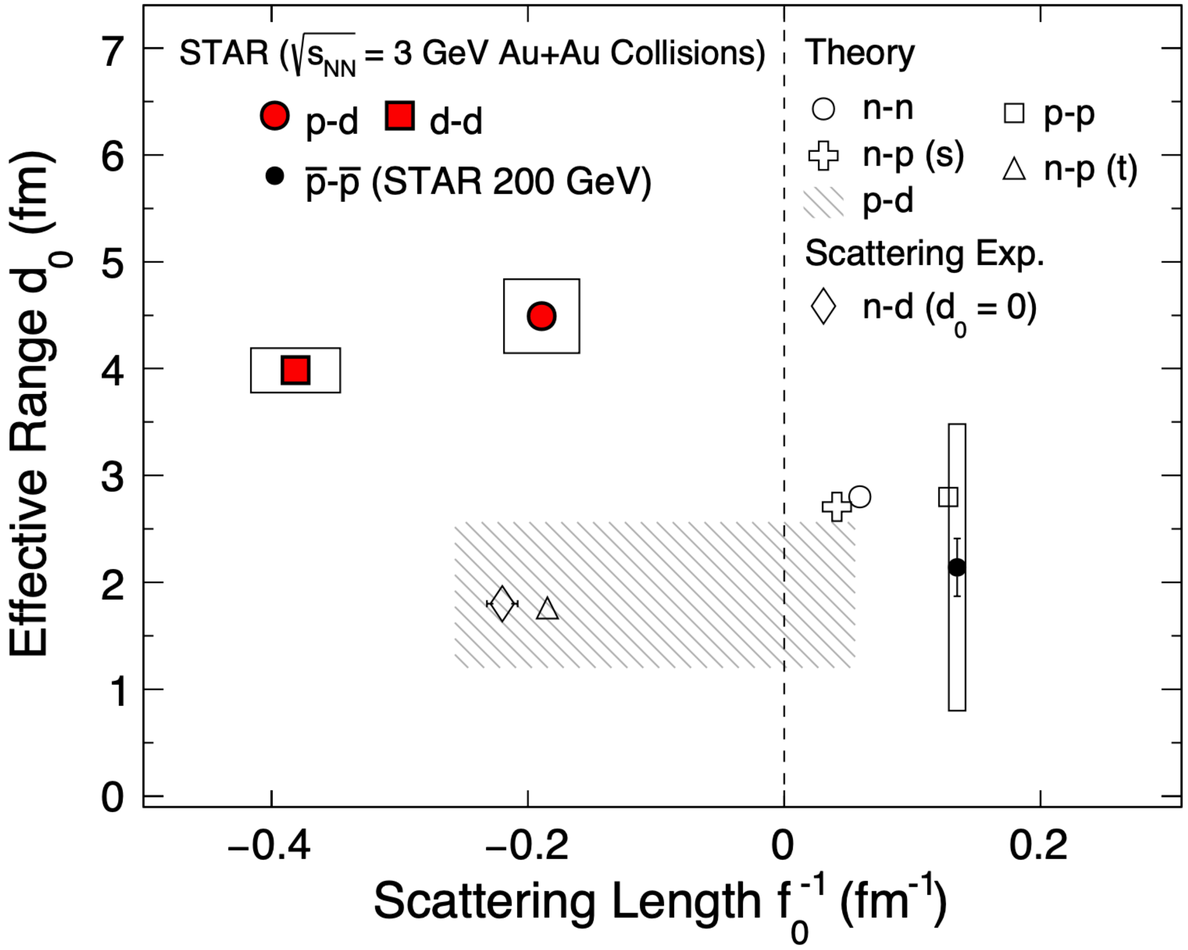

- For both p-d and d-d interaction, the spin-averaged f_0 is negative
  - Combination of repulsive interactions in quartet (quintet) spin state for p-d (d-d) along with the presence of bound states (^{3}He for p-d and ^{4}He for d-d)
- For p-d interaction, the result is consistent with theory calculation and measurement in low-energy scattering experiment

STAR, arXiv: 2410.03436

d-Λ correlations

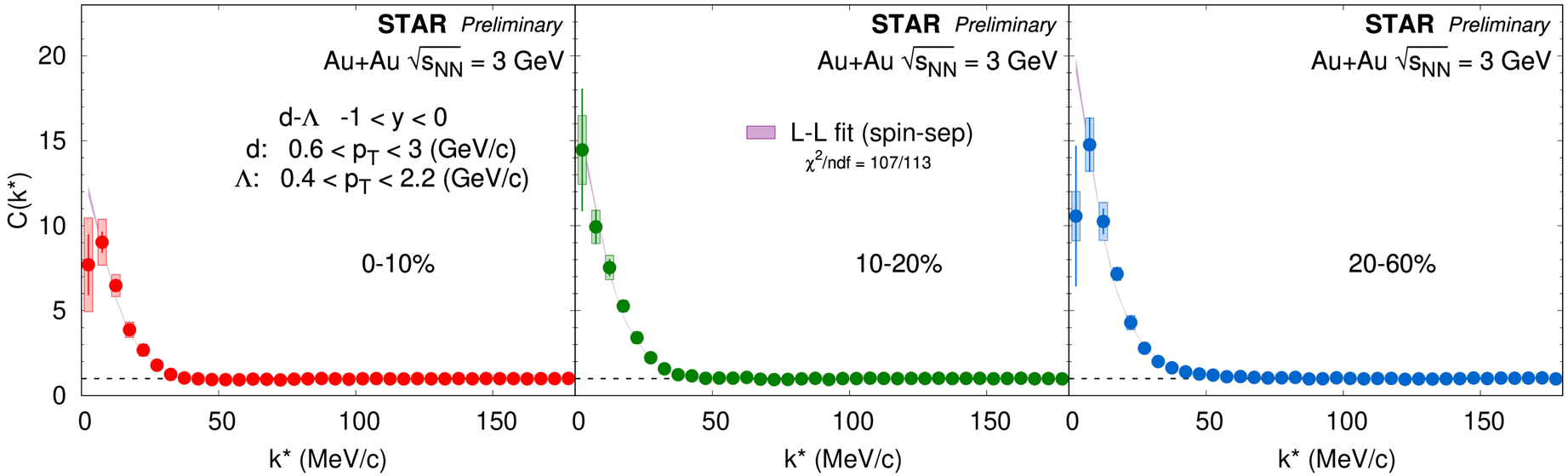

- First measurement of d-Λ correlations
- Strong enhancement at small k^* → attractive strong interactions
- Simultaneously fit to data in different centralities with L-L approach, consider two-spin components: D (doublet, S = 1/2), Q (quartet, S = 3/2)

$$|\Psi(r^*,k^*)|^2 = \frac{1}{3}|\Psi_{1/2}(r^*,k^*)|^2 + \frac{2}{3}|\Psi_{3/2}(r^*,k^*)|^2$$

EPJ Web Conf. **296** (2024) 14010

d-Λ correlations

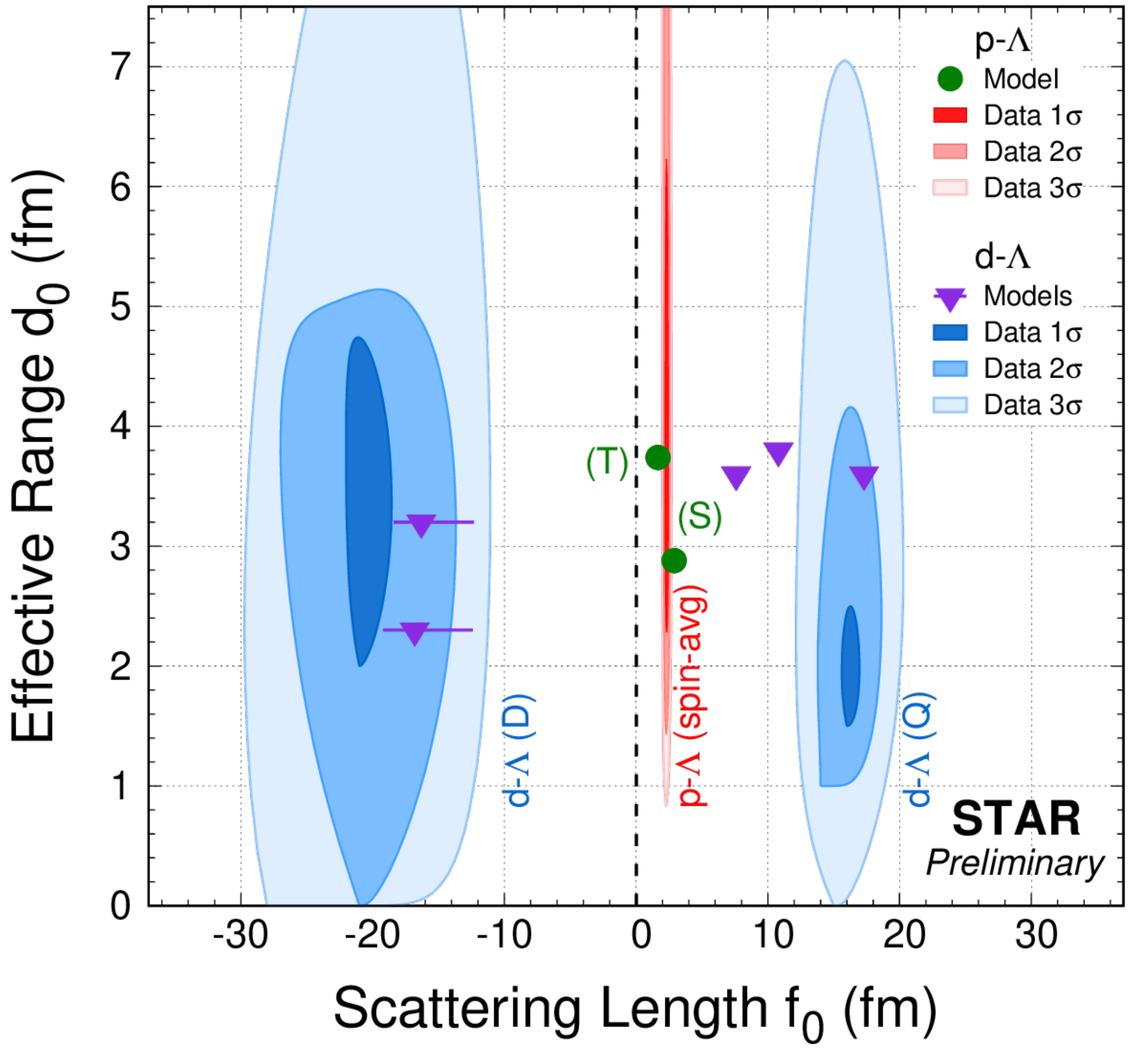

- Successfully separate two spin components in d-Λ
  - $f_0(D) = -20^{+3}_{-3}$ fm, $d_0(D) = 3^{+2}_{-1}$ fm
  - $f_0(Q) = 16^{+2}_{-1}$ fm, $d_0(Q) = 2^{+1}_{-1}$ fm
- Negative f_0 in doublet state → ${}^{3}_{\Lambda}\mathrm{H}$ bound state
- Positive f_0 in quartet state → attractive interaction

EPJ Web Conf. **296** (2024) 14010

d-Λ correlations

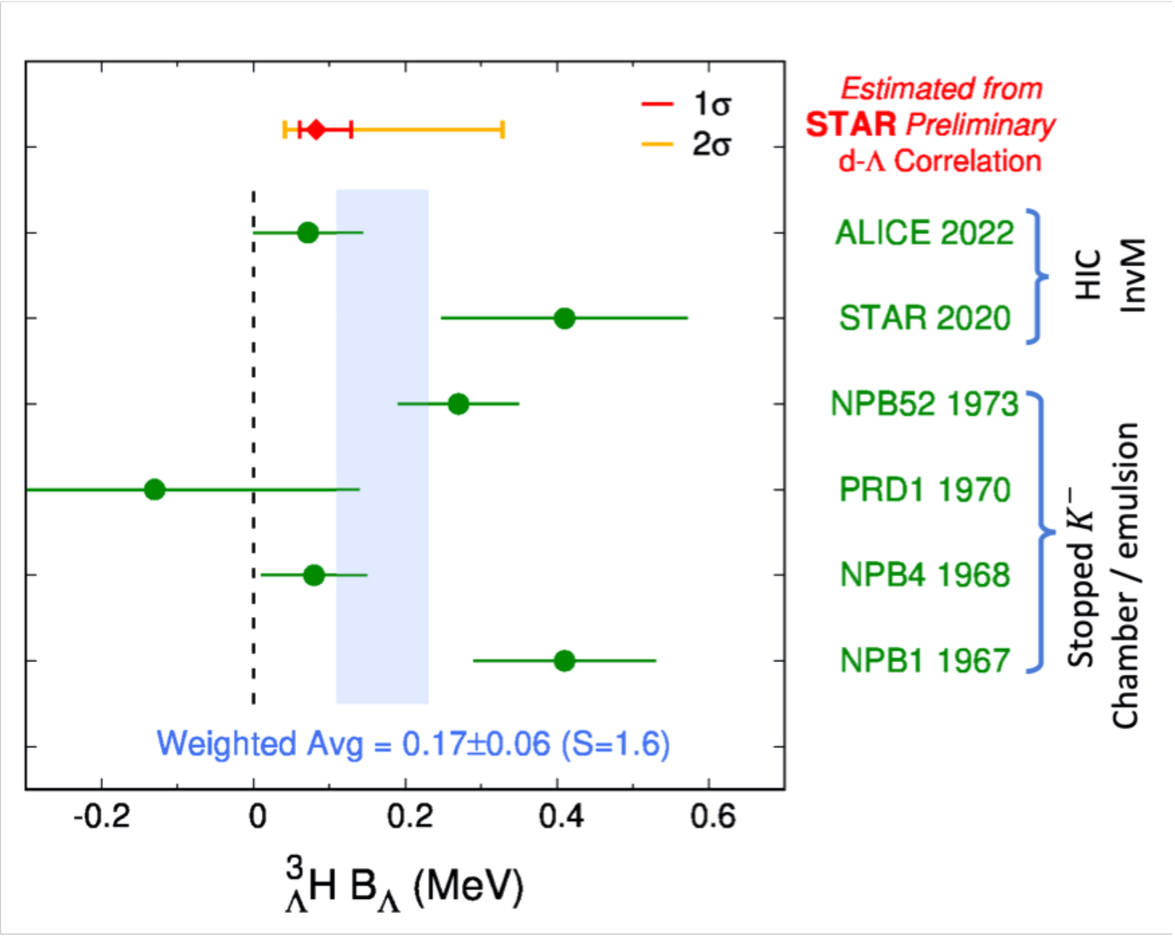

- $^3_\Lambda\mathrm{H}$ binding energy (B_Λ): Bethe formula from Effective Range Expansion

$$B_\Lambda = \frac{\gamma^2}{2\mu_{d\Lambda}}, \frac{1}{-f_0} = \gamma - \frac{1}{2} d_0 \gamma^2$$

$\mu_{d\Lambda}$: reduced mass, γ: binding momentum

- $^3_\Lambda\mathrm{H}$ B_Λ = [0.04, 0.33] MeV (95% CL)
  - Consistent with world average
  - New way to constrain $^3_\Lambda\mathrm{H}$ properties

H.Bethe, Phys. Rev **76** (1949) 38
EPJ Web Conf. **296** (2024) 14010

p-Ξ^- correlations

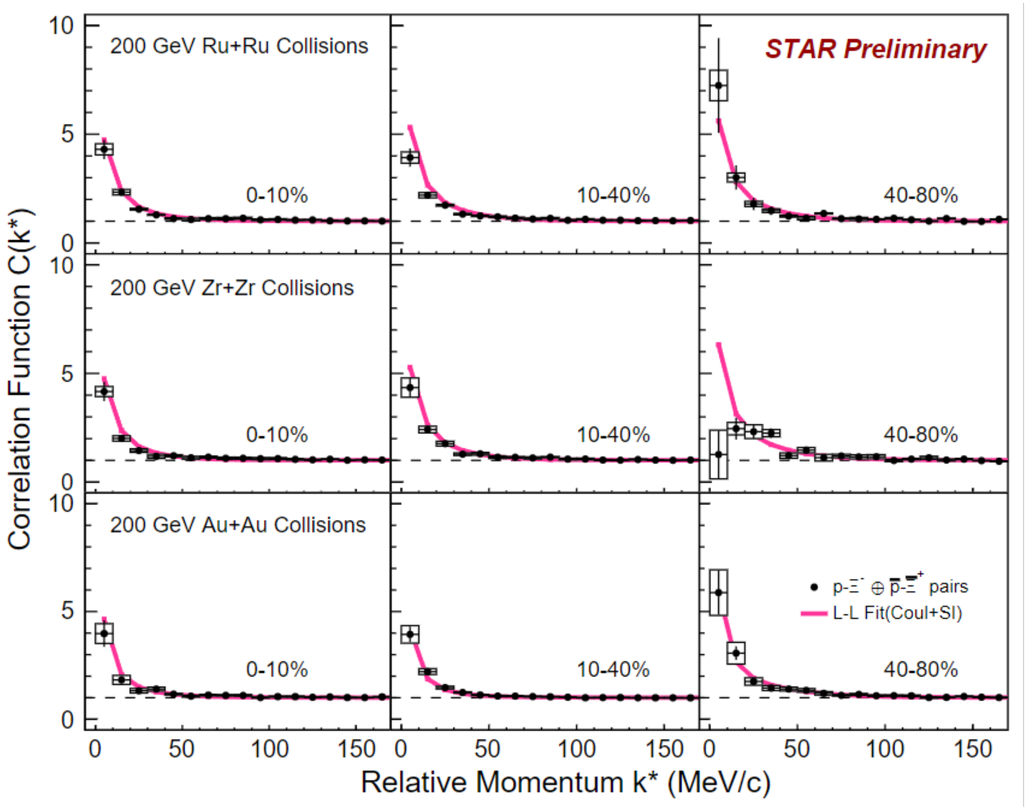

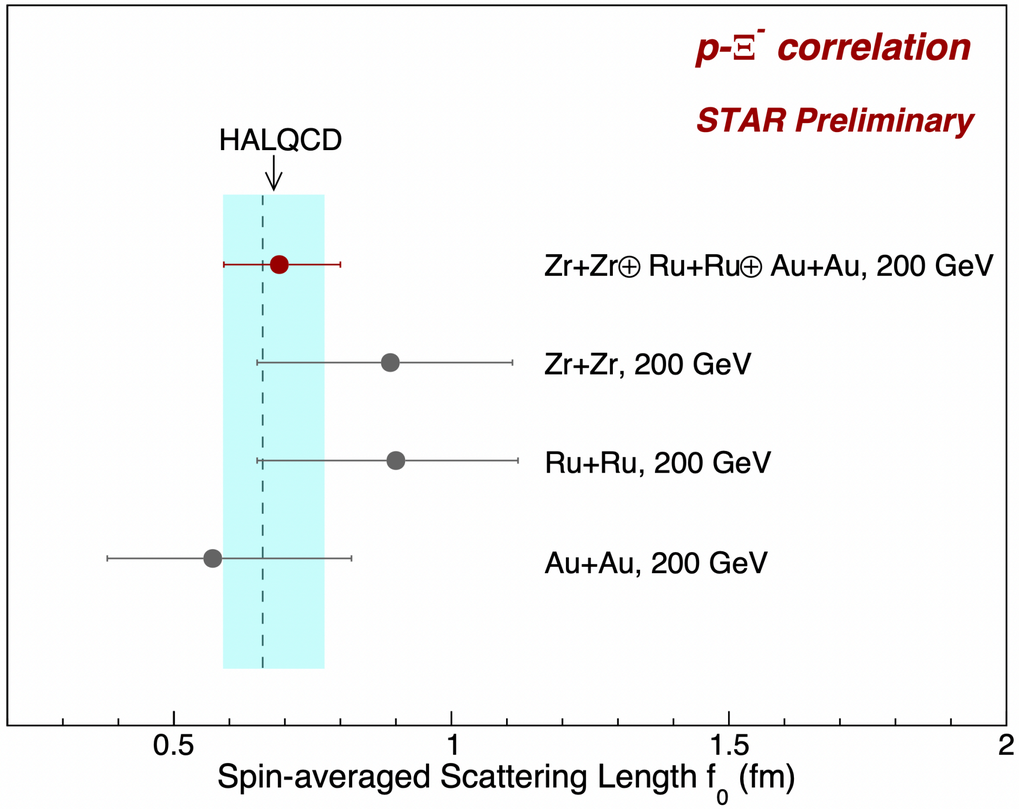

- Enhancement at small k^*
  - Due to Coulomb attraction and strong interactions

- First measurement of strong interaction parameters of p-Ξ^-
  - Shallow attractive interaction
- f_0 is consistent with HALQCD prediction

p-Ω^- correlations

Spin-2 pOmega potentials	VI	VII	VIII
Binding energy E_B (MeV)	-	6.3	26.9
Scattering length a_0 (fm)	-1.12	5.79	1.29
Effective range r_eff (fm)	1.16	0.96	0.65
	No bound state	Shallow bound	Deep bound

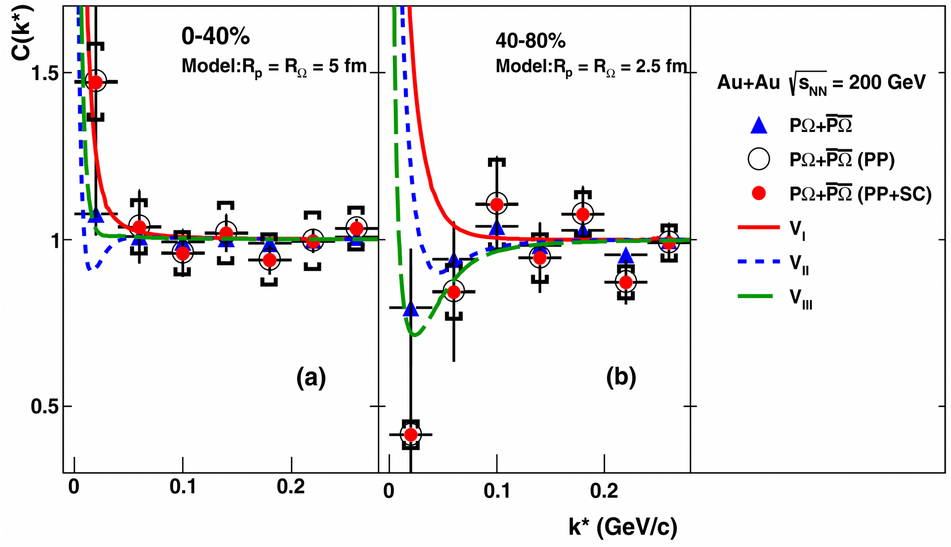

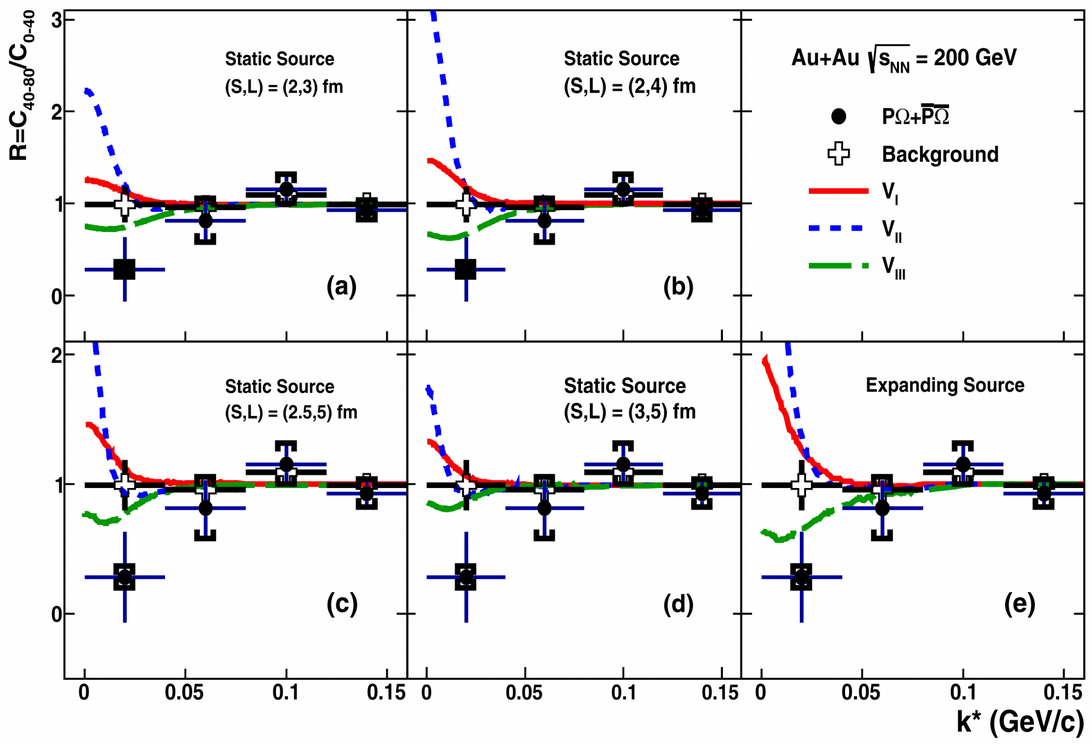

- Experimental p-Ω^- correlation functions favour V_{III} potential
  - Existence of bound state is supported

K. Morita *et al.* PRC **94** (2016) 031901
STAR, Phys. Lett. B **790** (2019) 490

Λ-Λ correlations

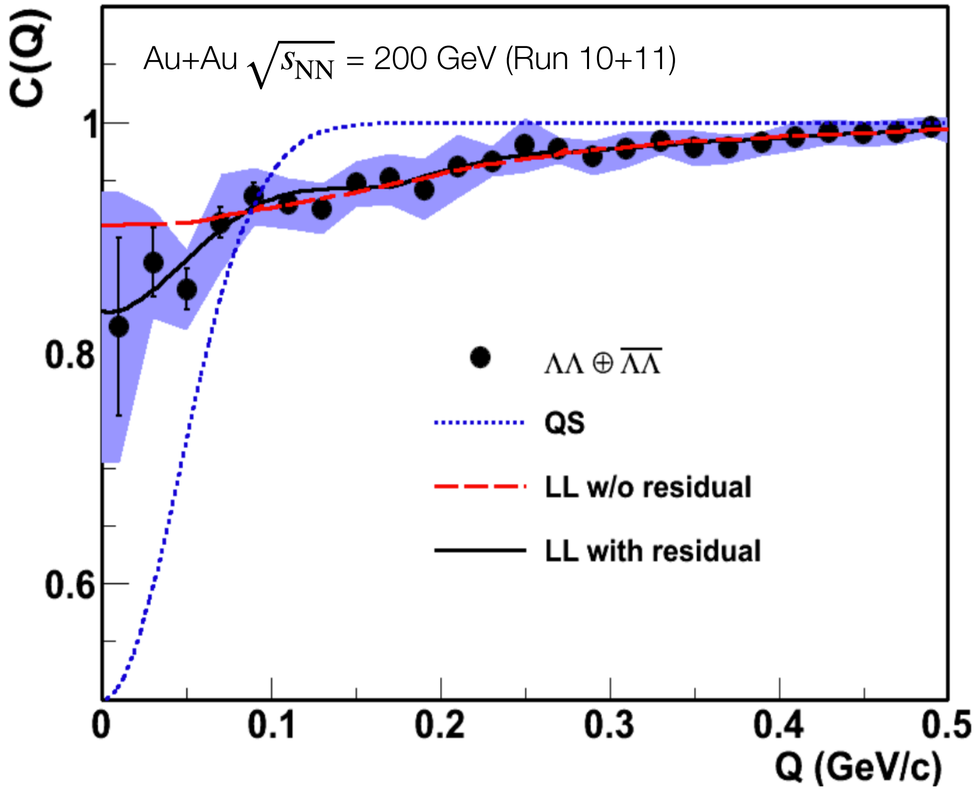

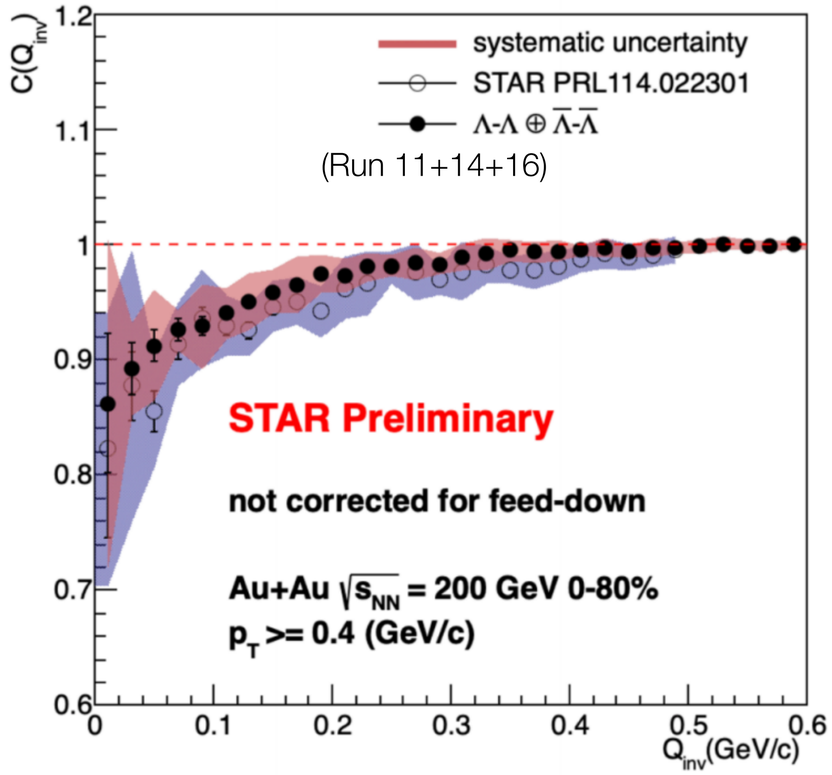

- Extracted paramaters from Lednický–Lyuboshitz model fit:
  - $f_0 = -1.1 \pm 0.37^{+0.68}_{-0.08}$, $d_0 = 8.56 \pm 2.56^{+2.09}_{-0.74}$
- Without feed-down correction

- Repeat analysis with increased statistics by factor of 4
  - More detailed study is needed

STAR, PRL **114** (2015) 022301
EPJ Web Conf. 259 (2022) 11015

Summary

- Extraction of emitting source using femtoscopy:
  - Femtoscopic source size is measured over a wide range of collision energy
  - Dynamic properties of the source: emission time, source tilt angle, freeze-out eccentricity, space-time emission asymmetry, are determined
- Extraction of final state interaction using femtoscopy:
  - Powerful tool to measure of parameters of strong interactions, complement to scattering experiments
  - Extraction of parameters of strong interation of $\bar{p}$-$\bar{p}$, p-d, d-d, p-Λ, d-Λ, p-Ξ^-, p-Ω^-, Λ-Λ
  - Implications of possible bound states

Not all STAR femtoscopy results could be covered in this talk
Stay tuned for more STAR BES-II and FXT femtoscopy results